

INT-FLASHATTENTION: ENABLING FLASH ATTENTION FOR INT8 QUANTIZATION

Shimao Chen¹, Zirui Liu¹, Zhiying Wu², Ce Zheng³, Peizhuang Cong¹,
Zihan Jiang¹, Yuhan Wu¹, Lei Su², Tong Yang^{1*}

¹ Peking University, ² Baichuan Inc, ³ Beihang University.

ABSTRACT

As the foundation of large language models (LLMs), self-attention module faces the challenge of quadratic time and memory complexity with respect to sequence length. FlashAttention accelerates attention computation and reduces its memory usage by leveraging the GPU memory hierarchy. A promising research direction is to integrate FlashAttention with quantization methods. This paper introduces INT-FlashAttention, the first INT8 quantization architecture compatible with the forward workflow of FlashAttention, which significantly improves the inference speed of FlashAttention on Ampere GPUs. We implement our INT-FlashAttention prototype with fully INT8 activations and general matrix-multiplication (GEMM) kernels, making it the first attention operator with fully INT8 input. As a general token-level post-training quantization framework, INT-FlashAttention is also compatible with other data formats like INT4, *etc.* Experimental results show INT-FlashAttention achieves 72% faster inference speed and 82% smaller quantization error compared to standard FlashAttention with FP16 and FP8 data format. All related codes are open-sourced ¹.

1 INTRODUCTION

Large language models (LLMs), such as GPT Achiam et al. (2023) and Llama Touvron et al. (2023), have achieved significant breakthroughs across various domains. Self-attention module is the foundation of LLMs, allowing them to capture dependencies between different tokens in a sequence Vaswani et al. (2017). However, the computation of self-attention module entails quadratic time and memory complexity with respect to the sequence length, which hinders the scaling of LLMs to longer contexts. To address this bottleneck, Dao et al. propose excellent FlashAttention Dao et al. (2022), which exploits the GPU memory hierarchy to design a tiling strategy to speed up the attention computation and reduce memory from quadratic to linear w.r.t. sequence length.

Another popular method of improving the computational performance and memory usage of LLMs is to reduce the bit size of the floating-point data used in these models, which is a technique known as model quantization. Modern hardware incorporates advanced Tensor Cores to support efficient general matrix-multiplication (GEMM) for FP16, FP8 Micikevicius et al. (2022), and INT8 van Baalen et al. (2023). Quantization methods make full use of these dedicated computing units to improve the spatiotemporal efficiency of LLMs by compressing the parameters and activations into FP8, INT8, and even ternary format. Existing quantization methods can be broadly divided into two categories: quantization during training and post-training quantization. This paper focuses on the latter, utilizing quantization to enhance LLM inference efficiency.

Integrating FlashAttention with quantization methods is a promising research direction. Designed for the most advanced NVIDIA Hopper GPUs, the latest FlashAttention-3 Shah et al. (2024) already supports FP8 data format. Unfortunately, NVIDIA Ampere series GPUs, such as A100, do not provide hardware support for FP8. While Hopper architecture significantly enhances both computational power and energy efficiency, existing Ampere architecture still holds a substantial share in the data center GPU market. According to available data, A100 GPUs are still estimated to contribute

*Corresponding author: Tong Yang (yangtong@pku.edu.cn)

¹<https://github.com/INT-FlashAttention2024/INT-FlashAttention>

approximately 20% of the total compute power in accelerated supercomputers Morgan (2024). This dominance is largely due to their extensive deployment across numerous data centers worldwide. Given that the Ampere architecture provides computational support for INT8 data format, this paper aims to develop a fully INT8 version of FlashAttention, significantly improving the inference speed of FlashAttention on Ampere GPUs compared to the basic FlashAttention with FP16.

Towards the above design goal, we propose INT-FlashAttention, a novel token-level post-training quantization architecture designed to align with the computation workflow of FlashAttention. We implement our INT-FlashAttention prototype with INT8-type \mathbf{Q} , \mathbf{K} , and \mathbf{V} matrices. We use INT8 general matrix-multiplication (GEMM) kernels to replace all matrix multiplications during inference, thus significantly improving inference speed and saving energy. To the best of our knowledge, we are the first to develop the attention operator with fully INT8 inputs. By preserving token-level information, INT-FlashAttention offers a substantial accuracy improvement over existing tensor-level FP8 methods Shah et al. (2024). Last but not least, our token-level quantization method is not limited to INT8 format, which can also be adapted to other data formats like INT4, and *etc.* Experimental results show that the INT8 version of INT-FlashAttention achieves 72% faster inference speed compared to FlashAttention-FP16 and up to 82% smaller quantization error compared to FlashAttention-FP8.

This paper makes the following contributions:

- We propose INT-FlashAttention, a token-level post-training quantization architecture that can be seamlessly integrated with the forward workflow of FlashAttention.
- We implement the INT8 version of our INT-FlashAttention prototype, which is the first attention operator with fully INT8 input (to the best of our knowledge).
- We conduct experiments evaluating the performance of INT-FlashAttention, showing that it achieves significantly faster inference speed and higher quantization accuracy than baseline solutions.

2 BACKGROUND AND RELATED WORK

2.1 STANDARD ATTENTION

Given input sequence $\mathbf{Q}, \mathbf{K}, \mathbf{V} \in \mathbb{R}^{N \times d}$, where N is the sequence length and d is the head dimension, standard attention computes the attention output $\mathbf{O} \in \mathbb{R}^{N \times d}$:

$$\mathbf{S} = \mathbf{Q}\mathbf{K}^T \in \mathbb{R}^{N \times N}, \mathbf{P} = \text{softmax}(\mathbf{S}) \in \mathbb{R}^{N \times N}, \mathbf{O} = \mathbf{P}\mathbf{V} \in \mathbb{R}^{N \times d},$$

where softmax is applied row-wise. Here, we call \mathbf{S} *attention score matrix* and call \mathbf{P} *attention weight matrix*.

Standard attention implements the intermediate matrices \mathbf{S} and \mathbf{P} to HBM, which takes $O(N^2)$ memory. During forward computation, standard attention implementation first loads the entire inputs from GPU high bandwidth memory (HBM), calculates $\mathbf{S} = \mathbf{Q}\mathbf{K}^T$ and writes \mathbf{S} back to HBM. Then it loads \mathbf{S} from HBM, calculates $\mathbf{P} = \text{softmax}(\mathbf{S})$, and writes \mathbf{P} back to HBM. It finally calculates $\mathbf{O} = \mathbf{P}\mathbf{V}$ to get the final results. We can see that in the circumstance above, most of the operations are bounded by the HBM bandwidth, and thus the large number of memory accesses dominates the time taken by attention operations.

2.2 FLASHATTENTION FAMILIES

To speed up attention on hardware accelerators with hierarchical memory, FlashAttention Dao (2023) proposes to use the tiling techniques to reduce memory reads/writes and fuse the attention operations into a single kernel. Specifically, FlashAttention divides the input sequences into smaller blocks. During the forward computation, it first loads blocks of inputs from HBM to SRAM, computes attention for each block and then updates the output without writing the large intermediate matrices \mathbf{S} and \mathbf{P} back to HBM. Since the softmax function in the attention mechanism needs to be applied to the entire row, FlashAttention employs an online softmax method Milakov & Gimelshein (2018); Rabe & Staats (2021) to split the computation into blocks and finally rescale the output

of each block to obtain the correct result. Built on FlashAttention, FlashAttention-2 Dao (2023) modifies the design of the inner loop in the forward pass and introduces two tweaks to reduce non-matmul FLOPs, thereby improving GPU occupancy. FlashAttention-3 Shah et al. (2024) further leverages Tensor Cores and TMA asynchrony to optimize the FlashAttention implementation on Hopper GPUs. In particular, it utilizes block quantization and the hardware support for FP8 low-precision to implement an FP8 version of FlashAttention on Hopper GPUs.

2.3 MODEL QUANTIZATION

LLM quantization. Recent years have witnessed a great surge in applying various quantization methods to reduce the memory and energy consumption of LLMs. Quantization methods compress the parameters from standard FP32 to continuous FP16 Dao et al. (2022), FP8 Shah et al. (2024); Lee et al. (2024), discrete INT8 Dettmers et al. (2022), and even ternary formats Chen et al. (2024). Many studies suggest that INT8 consumes significantly less memory for loading model weights and requires less energy than the FP8 and FP16 counterparts Dally (2015); van Baalen et al. (2023). The naive LLM quantization approaches adopt tensor-level quantization Zhou et al. (2024). However, many studies found that the weight distributions vary significantly across different tokens, and the existence of activation outliers makes LLM difficult to quantize at whole-tensor level Tao et al. (2022); Xu et al. (2024). As a result, many works adopted token-level or block-level quantization methods to improve model accuracy Zhou et al. (2024); Li et al. (2024). The most recent FlashAttention-3 Shah et al. (2024) adopts a block-level FP8 quantization method. However, to the best of our knowledge, there is no existing work that integrates token-level quantization with FlashAttention, neither is there a version of FlashAttention that supports INT8 data format.

Post-training quantization. There is a line of post-training quantization (PTQ) strategies for effectively reducing model sizes and improving the inference speed of LLMs. Some work design custom quantization blocks to improve quantization accuracy Dettmers et al. (2022); Li et al. (2021). Other works use feature segmentation strategies to protect the outlier features so as to reduce the quantization error Shang et al. (2023); Dettmers et al. (2023). GPTQ Frantar et al. (2022) designs a more accurate one-shot quantization framework based on approximate second-order information Frantar & Alistarh (2022), achieving good accuracy in extreme low-bit quantization regime (2-bit). Subsequent works propose to identify and select salient weights and preserve their information through scaling transformations Lee et al. (2023) or residual approximation Huang et al. (2024).

3 THE INT-FLASHATTENTION ARCHITECTURE

Developed based on FlashAttention Dao et al. (2022), INT-FlashAttention implements the \mathbf{Q} , \mathbf{K} , and \mathbf{V} matrices in fully INT8 format (colored green in Figure 1) with token-level quantization. We use the INT8 general matrix multiplication (GEMM) kernel to replace all matrix multiplications in FlashAttention (originally in FP16/FP8 format). Due to the efficient INT8 compression, INT-FlashAttention can read larger blocks from HBM per iteration compared to basic FlashAttention with FP16 format. Additionally, the INT8 matrix multiplication operators in INT-FlashAttention also outperform their floating-point counterparts. As a result, INT-FlashAttention achieves notable improvement in inference speed compared to basic FlashAttention. Furthermore, with per-token quantization, INT-FlashAttention offers better inference accuracy than the FP8 version of FlashAttention-3 Shah et al. (2024) with tensor-level quantization.

In this section, we first introduce the workflow of the online softmax operation in Section 3.1, which forms the foundation of both FlashAttention and INT-FlashAttention. Then we explain how INT-FlashAttention seamlessly integrates INT8 quantization into the online softmax workflow in Section 3.2.

3.1 PRELIMINARY OF ONLINE SOFTMAX

We first describe the workflow of the online softmax method Milakov & Gimelshein (2018); Rabe & Staats (2021) in detail, which is the base of FlashAttention Dao et al. (2022) and our INT-FlashAttention. As shown in Figure 1 and Algorithm 1, in the forward workflow of FlashAttention (also our INT-FlashAttention), we iterate over blocks of the input \mathbf{Q} and \mathbf{K}/\mathbf{V} matrices. For each iteration in the outer loop (line 4-5 in Algorithm 1), we load a block \mathbf{Q}_i from HBM,

and then perform the inner loop over blocks of the \mathbf{K} and \mathbf{V} matrices. In each iteration of the inner loop (line 7-8 in Algorithm 1), we load the blocks \mathbf{K}_j and \mathbf{V}_j from HBM and compute $\mathbf{S}_i^{(j)} = \mathbf{Q}_i \mathbf{K}_j^T$. In standard attention, a row-wise softmax operation is required on the entire attention matrix $\mathbf{S}_i = [\mathbf{S}_i^{(1)} \mathbf{S}_i^{(2)} \dots \mathbf{S}_i^{(T_c)}]$. The online softmax method achieves the same result as standard attention by scaling the output of each inner loop iteration with the appropriate normalization factor.

For simplicity, consider there are only one-row block and two column blocks in the attention matrix $\mathbf{S} = [\mathbf{S}^{(1)} \mathbf{S}^{(2)}]$ where $\mathbf{S}^{(1)}, \mathbf{S}^{(2)} \in \mathbb{R}^{B_r \times B_c}$. We want to compute row-wise softmax on \mathbf{S} and multiply the result $\mathbf{P} = \text{softmax}(\mathbf{S})$ with the value $\mathbf{V} = \begin{bmatrix} \mathbf{V}^{(1)} \\ \mathbf{V}^{(2)} \end{bmatrix}$ where $\mathbf{V}^{(1)}, \mathbf{V}^{(2)} \in \mathbb{R}^{B_c \times d}$. Standard softmax computes as follows.

$$\begin{aligned} m &= \max(\text{rowmax}(\mathbf{S}^{(1)}), \text{rowmax}(\mathbf{S}^{(2)})) \in \mathbb{R}^{B_r} \\ l &= \text{rowsum}(e^{\mathbf{S}^{(1)}-m}) + \text{rowsum}(e^{\mathbf{S}^{(2)}-m}) \in \mathbb{R}^{B_r} \\ \mathbf{P} &= [\mathbf{P}^{(1)} \mathbf{P}^{(2)}] = \text{diag}(l)^{-1} \begin{bmatrix} e^{\mathbf{S}^{(1)}-m} & e^{\mathbf{S}^{(2)}-m} \end{bmatrix} \in \mathbb{R}^{B_r \times 2B_c} \\ \mathbf{O} &= [\mathbf{P}^{(1)} \mathbf{P}^{(2)}] \begin{bmatrix} \mathbf{V}^{(1)} \\ \mathbf{V}^{(2)} \end{bmatrix} = \text{diag}(l)^{-1} e^{\mathbf{S}^{(1)}-m} \mathbf{V}^{(1)} + e^{\mathbf{S}^{(2)}-m} \mathbf{V}^{(2)} \in \mathbb{R}^{B_r \times d} \end{aligned}$$

Online softmax computes local softmax within each block $\mathbf{S}^{(i)}$ and finally rescales the results to get the same output as standard softmax. The following formulas describe the online softmax implemented in FlashAttention-2 Dao (2023), which also forms the foundation of our INT-FlashAttention. We annotate these formulas with their corresponding line numbers in the pseudocode of Algorithm 1.

$$\begin{aligned} m^{(1)} &= \text{rowmax}(\mathbf{S}^{(1)}) \in \mathbb{R}^{B_r} \\ l^{(1)} &= \text{rowsum}(e^{\mathbf{S}^{(1)}-m^{(1)}}) \in \mathbb{R}^{B_r} \\ \tilde{\mathbf{O}}^{(1)} &= e^{\mathbf{S}^{(1)}-m^{(1)}} \mathbf{V}^{(1)} \in \mathbb{R}^{B_r \times d} \\ m^{(2)} &= \max(m^{(1)}, \text{rowmax}(\mathbf{S}^{(2)})) = m && \text{(Line 10)} \\ l^{(2)} &= e^{m^{(1)}-m^{(2)}} l^{(1)} + \text{rowsum}(e^{\mathbf{S}^{(2)}-m^{(2)}}) = l && \text{(Line 12)} \\ \tilde{\mathbf{O}}^{(2)} &= \text{diag}(e^{m^{(1)}-m^{(2)}}) \tilde{\mathbf{O}}^{(1)} + e^{\mathbf{S}^{(2)}-m^{(2)}} \mathbf{V}^{(2)} = e^{\mathbf{S}^{(1)}-m} \mathbf{V}^{(1)} + e^{\mathbf{S}^{(2)}-m} \mathbf{V}^{(2)} && \text{(Line 13)} \\ \mathbf{O}^{(2)} &= \text{diag}(l^{(2)})^{-1} \tilde{\mathbf{O}}^{(2)} = \mathbf{O} && \text{(Line 16).} \end{aligned}$$

From the formulas above, we can see that during the inner loop iterations, by real-time maintaining the current row-wise maximum values $m^{(j)}$ and the sum of exponentials $l^{(j)}$, and by finally rescaling the output, online softmax can attain the same output as standard softmax.

3.2 INT-FLASHATTENTION ATTENTION DESIGN

INT-FlashAttention implements the \mathbf{Q} , \mathbf{K} , and \mathbf{V} matrices in self-attention module with fully INT8 format. In Figure 1, we use green color to represent the data in INT8 format and the INT8 GEMM operations and use orange color to represent data and operations with FP32 format. The GEMM used in INT-FlashAttention takes two INT8 input matrices and produces an INT32 output matrix. As shown in Figure 1 and Algorithm 1, during inference workflow, all data stored in HBM (\mathbf{Q} , \mathbf{K} , and \mathbf{V}) and all matrix multiplication operations ($\mathbf{Q}_i \mathbf{K}_j^T$ and $\mathbf{P}_i^{(j)} \mathbf{V}_j$) are implemented with INT8 format.

We maintain two vector scalars $\mathbf{S}_Q, \mathbf{S}_K \in \mathbb{R}^N$, for token-level quantization of the \mathbf{Q} and \mathbf{K} matrices. For the \mathbf{V} matrix, we maintain a constant scalar $\mathbf{S}_V \in \mathbb{R}$ for tensor-level quantization². After training, we perform linear symmetric quantization on the \mathbf{Q} , \mathbf{K} , and \mathbf{V} matrices, quantizing them into INT8 format and obtaining scalars $\mathbf{S}_Q = \frac{\text{rowmax}(|\mathbf{Q}|)}{R}$, $\mathbf{S}_K = \frac{\text{rowmax}(|\mathbf{K}|)}{R}$, and $\mathbf{S}_V = \frac{\text{max}(|\mathbf{V}|)}{R}$, where $R = 256$ is the INT8 quantization range.

²We will implement \mathbf{V} on a per-block quantization basis in our future work.

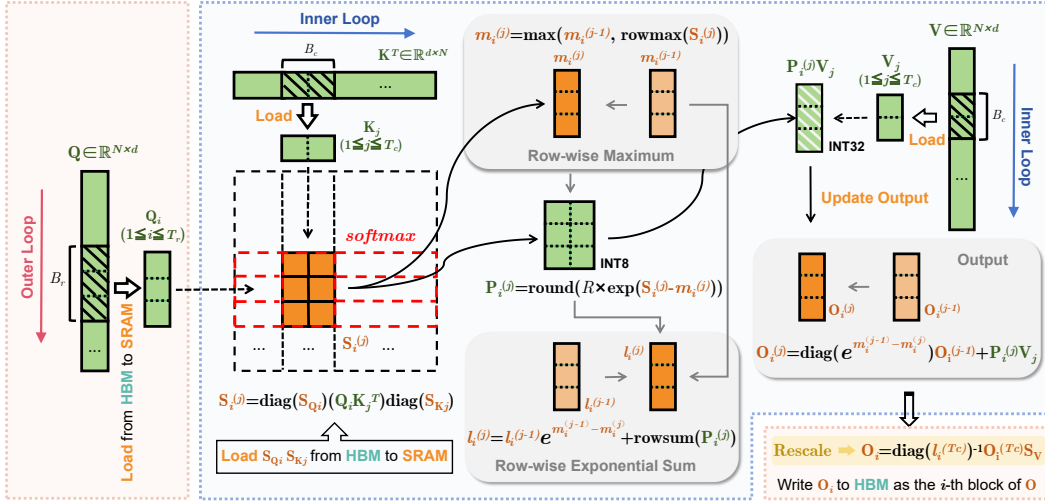


Figure 1: A single iteration in the inner loop of INT-FlashAttention forward pass (Algorithm 1), where green color represents INT8 data format and orange color represents FP32 data format.

As described in Algorithm 1, the attention forward workflow of INT-FlashAttention is similar to FlashAttention-2. Besides dividing \mathbf{Q} , \mathbf{K} , \mathbf{V} , and \mathbf{O} into blocks (line 1-2), we also divide scalars \mathbf{S}_Q and \mathbf{S}_K into blocks (line 3). The outer loop iterates over each block \mathbf{Q}_i of matrix \mathbf{Q} (line 4-5). For each block \mathbf{Q}_i , we also maintain the current row-wise maximum values $m_i^{(j)}$ and the sum of modified exponentials $l_i^{(j)}$ (explained later). Both $m_i^{(j)}$ and $l_i^{(j)}$ are of FP32 format.

Figure 1 illustrates an iteration in the inner loop, which iterates over each block \mathbf{K}_j and \mathbf{V}_j of matrix \mathbf{K} and \mathbf{V} (line 7-8). We first call the integer GEMM kernel (with INT8 input and INT32 output) to multiply \mathbf{Q}_i and \mathbf{K}_j , and then scale the result with \mathbf{S}_{Q_i} and \mathbf{S}_{K_j} to get the attention score matrix $\mathbf{S}_i^{(j)}$ with FP32 format (line 9). Thanks to the linearity of integer multiplication, the resulting attention score matrix $\mathbf{S}_i^{(j)}$ is equivalent to the standard attention score matrix obtained by first scaling \mathbf{Q}_i and \mathbf{K}_j with \mathbf{S}_{Q_i} and \mathbf{S}_{K_j} , and then performing matrix multiplication with FP32 GEMM kernel on $(\text{diag}(\mathbf{S}_{Q_i}) \mathbf{Q}_i)$ and $(\mathbf{K}_j^T \text{diag}(\mathbf{S}_{K_j}))$. We update row-wise maximum values $m_i^{(j)}$ with $\mathbf{S}_i^{(j)}$ (line 10).

For the attention weight matrix $\mathbf{P}_i^{(j)}$, we aim to quantize it into INT8 format, allowing us to directly use INT8 GEMM for the $\mathbf{P}_i^{(j)} \mathbf{V}_j$ computation to update output (line 13). According to the formulas in Section 3.1, standard FlashAttention would compute $\tilde{\mathbf{P}}_i^{(j)} = \exp(\mathbf{S}_i^{(j)} - m_i^{(j)}) \in (0, 1]^{B_r \times B_c}$ (line 11) and $l_i^{(j)} = l_i^{(j-1)} e^{m_i^{(j-1)} - m_i^{(j)}} + \text{rowsum}(\tilde{\mathbf{P}}_i^{(j)}) \in \mathbb{R}^{B_r}$ (line 12). As the values in $\tilde{\mathbf{P}}_i^{(j)}$ already falls between $(0, 1]$, we directly use $\mathbf{S}_P = \frac{1}{R}$ as the scaling factor for $\tilde{\mathbf{P}}_i^{(j)}$ and compute $\mathbf{P}_i^{(j)} = \text{round}(\tilde{\mathbf{P}}_i^{(j)} / \mathbf{S}_P) = \text{round}(R \times \exp(\mathbf{S}_i^{(j)} - m_i^{(j)})) \in \mathbb{I}_8^{B_r \times B_c}$ (line 11). Then we directly use the quantized weight matrix $\mathbf{P}_i^{(j)}$ to update the sum of exponentials $l_i^{(j)}$, thereby implicitly dividing the scaling factor \mathbf{S}_P into $l_i^{(j)}$ (line 12). At the end of every iteration of the outer loop, we scale the final $\mathbf{O}_i^{(T_c)}$ with $\text{diag}(l_i^{(T_c)})^{-1}$ to get the right output (line 16). In this process, we implicitly multiplied the scaling factor \mathbf{S}_P into the output, completing the dequantization from integer to float. Finally, we return the right output \mathbf{O} , which is equivalent to the output matrix calculated with standard softmax function and float computations.

Algorithm 1 INT-FlashAttention Attention Forward

Require: Matrices $\mathbf{Q}, \mathbf{K}, \mathbf{V} \in \mathbb{I}_8^{N \times d}$ ($\mathbb{I}_8 := [-128, 127] \cap \mathbb{Z}$ is the range of INT8), scalars $\mathbf{S}_\mathbf{Q}, \mathbf{S}_\mathbf{K} \in \mathbb{R}^N, \mathbf{S}_\mathbf{V} \in \mathbb{R}$ in HBM, block sizes B_c, B_r , INT8 maximum $R = 127$.

- 1: Divide \mathbf{Q} into $T_r = \lceil \frac{N}{B_r} \rceil$ blocks $\mathbf{Q}_1, \dots, \mathbf{Q}_{T_r}$, each have size $B_r \times d$, and divide \mathbf{K}, \mathbf{V} into $T_c = \lceil \frac{N}{B_c} \rceil$ blocks $\mathbf{K}_1, \dots, \mathbf{K}_{T_c}$ and $\mathbf{V}_1, \dots, \mathbf{V}_{T_c}$, each have size $B_c \times d$.
 - 2: Divide output $\mathbf{O} \in \mathbb{R}^{N \times d}$ into T_r blocks $\mathbf{O}_1, \dots, \mathbf{O}_{T_r}$, each have size $B_r \times d$.
 - 3: Divide $\mathbf{S}_\mathbf{Q}$ into T_r blocks $\mathbf{S}_{\mathbf{Q}_1}, \dots, \mathbf{S}_{\mathbf{Q}_{T_r}}$, each have size B_r , and divide $\mathbf{S}_\mathbf{K}$ into T_c blocks $\mathbf{S}_{\mathbf{K}_1}, \dots, \mathbf{S}_{\mathbf{K}_{T_c}}$, each have size B_c .
 - 4: **for** $1 \leq i \leq T_r$ **do**
 - 5: Load \mathbf{Q}_i and $\mathbf{S}_{\mathbf{Q}_i} \in \mathbb{R}^{B_r}$ from HBM to on-chip SRAM.
 - 6: On chip, initialize $\mathbf{O}_i^{(0)} = (0)_{B_r \times d}, l_i^{(0)} = (0)_{B_r}, m_i^{(0)} = (-\infty)_{B_r}$.
 - 7: **for** $1 \leq j \leq T_c$ **do**
 - 8: Load $\mathbf{K}_j, \mathbf{V}_j, \mathbf{S}_{\mathbf{K}_j} \in \mathbb{R}^{B_c}$ from HBM to on-chip SRAM.
 - 9: On chip, compute $\mathbf{S}_i^{(j)} = \text{diag}(\mathbf{S}_{\mathbf{Q}_i}) (\mathbf{Q}_i \mathbf{K}_j^T) \text{diag}(\mathbf{S}_{\mathbf{K}_j}) \in \mathbb{R}^{B_r \times B_c}$.
 - 10: On chip, compute $m_i^{(j)} = \max(m_i^{(j-1)}, \text{rowmax}(\mathbf{S}_i^{(j)})) \in \mathbb{R}^{B_r}$.
 - 11: On chip, compute $\mathbf{P}_i^{(j)} = \text{round}(R \times \exp(\mathbf{S}_i^{(j)} - m_i^{(j)})) \in \mathbb{I}_8^{B_r \times B_c}$ (pointwise).
 - 12: On chip, compute $l_i^{(j)} = l_i^{(j-1)} e^{m_i^{(j-1)} - m_i^{(j)}} + \text{rowsum}(\mathbf{P}_i^{(j)}) \in \mathbb{R}^{B_r}$.
 - 13: On chip, compute $\mathbf{O}_i^{(j)} = \text{diag}(e^{m_i^{(j-1)} - m_i^{(j)}}) \mathbf{O}_i^{(j-1)} + \mathbf{P}_i^{(j)} \mathbf{V}_j$
 - 14: **end for**
 - 15: Load $\mathbf{S}_\mathbf{V} \in \mathbb{R}$ from HBM to on-chip SRAM
 - 16: On chip, compute $\mathbf{O}_i = \text{diag}(l_i^{(T_c)})^{-1} \mathbf{O}_i^{(T_c)} \mathbf{S}_\mathbf{V}$.
 - 17: Write \mathbf{O}_i to HBM as the i -th block of \mathbf{O} .
 - 18: **end for**
 - 19: Return the output \mathbf{O} .
-

Specifically, as in Section 3.1, consider there are only one-row block and two column blocks in the attention matrix $\mathbf{S} = [\mathbf{S}^{(1)} \ \mathbf{S}^{(2)}]$ where $\mathbf{S}^{(1)}, \mathbf{S}^{(2)} \in \mathbb{R}^{B_r \times B_c}$. We have

$$m^{(1)} = \text{rowmax}(\mathbf{S}^{(1)}) \in \mathbb{R}^{B_r}$$

$$\mathbf{P}^{(1)} = \text{round}(R \times \exp(\mathbf{S}^{(1)} - m^{(1)}))$$

$$l^{(1)} = \text{rowsum}(\mathbf{P}^{(1)}) \in \mathbb{R}^{B_r}$$

$$\tilde{\mathbf{O}}^{(1)} = \mathbf{P}^{(1)} \mathbf{V}^{(1)} \in \mathbb{R}^{B_r \times d}$$

$$m^{(2)} = \max(m^{(1)}, \text{rowmax}(\mathbf{S}^{(2)})) = m \tag{Line 10}$$

$$\mathbf{P}^{(2)} = \text{round}(R \times \exp(\mathbf{S}^{(2)} - m^{(2)})) \tag{Line 11}$$

$$l^{(2)} = e^{m^{(1)} - m^{(2)}} l^{(1)} + \text{rowsum}(\mathbf{P}^{(2)}) = R \times l \tag{Line 12}$$

$$\tilde{\mathbf{O}}^{(2)} = \text{diag}(e^{m^{(1)} - m^{(2)}}) \tilde{\mathbf{O}}^{(1)} + \mathbf{P}^{(1)} \mathbf{V}^{(2)} = R \times e^{\mathbf{S}^{(1)} - m} \mathbf{V}^{(1)} + R \times e^{\mathbf{S}^{(2)} - m} \mathbf{V}^{(2)} \tag{Line 13}$$

$$\mathbf{O}^{(2)} = \text{diag}(l^{(2)})^{-1} \tilde{\mathbf{O}}^{(2)} = \frac{1}{R} \times \text{diag}(l)^{-1} \times (R \times e^{\mathbf{S}^{(1)} - m} \mathbf{V}^{(1)} + R \times e^{\mathbf{S}^{(2)} - m} \mathbf{V}^{(2)}) = \mathbf{O} \tag{Line 16}.$$

Notice that in the above formulas, we neglect the small errors introduced by integer rounding.

4 EMPIRICAL EVALUATION

We evaluate the inference speed and quantization accuracy of INT-FlashAttention, and compare it to FlashAttention with FP16 Dao (2023) and FP8 Shah et al. (2024) data format. We also compare

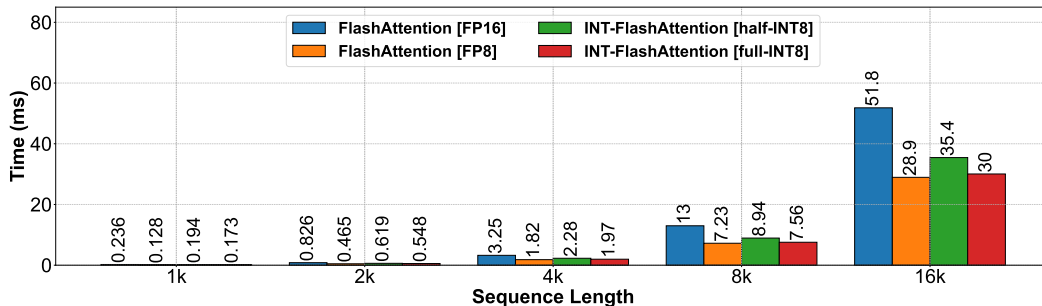


Figure 2: Comparison of inference speed.

INT-FlashAttention with a half-INT8 version of INT-FlashAttention with INT8-format \mathbf{Q} and \mathbf{V} matrices and FP16-format \mathbf{V} matrix. The experiments are conducted on an NVIDIA RTX4090 GPU. We highlight the following experimental results.

Inference speed. INT-FlashAttention achieves about 72% faster inference speed compared to FlashAttention with FP16 data format.

Quantization accuracy. INT-FlashAttention achieves about 46% and 82% smaller quantization error than FlashAttention with FP8 data format under normal-distributed and uniform-distributed activations, respectively.

4.1 INFERENCE SPEED

We implement INT-FlashAttention and the other candidate solutions in Triton, where we fix their batch size, number of heads, and dimension size per head to be the same. We evaluate the inference time with different context length. As shown in Figure 2, compared to standard FlashAttention with FP16 data format, INT-FlashAttention achieve 31%, 52%, 66%, 72%, and 73% smaller inference time under the sequence length of 1k, 2k, 4k, 8k, and 16k, respectively. We also notice that the inference time gap between INT-FlashAttention and FlashAttention-FP16 becomes larger as sequence length increases. On the other hand, INT-FlashAttention has nearly the same inference speed than FlashAttention with FP8 data format, with the gap narrowing as sequence length increases.

4.2 QUANTIZATION ACCURACY

We compare the quantization accuracy of INT-FlashAttention with the other candidate solutions. We manually create a one-layer self-attention module with the activations in its \mathbf{Q} , \mathbf{K} , and \mathbf{V} matrices following normal distribution $\mathcal{N}(0, 1)$ or uniform distribution $\mathcal{U}(-0.5, 0.5)$. We evaluate model quantization accuracy by measuring the Mean Relative Error (MRE) between original activations and activations after quantization and subsequent restoration. As shown in Table 1, under normal-distributed activations, INT-FlashAttention achieves up to $1.8\times$ smaller MRE compared to FlashAttention with FP8 data format. As shown in Table 2, under uniform-distributed activations, INT-FlashAttention achieves up to $5.6\times$ smaller MRE compared to FlashAttention with FP8 data format.

Table 1: Mean Relative Error (MRE) under normal-distributed activations.

Sequence Length	FlashAttention [FP8]	INT-FlashAttention [half-INT8]	INT-FlashAttention [full-INT8]
1k	7.46%	0.890%	4.05%
2k	7.50%	0.802%	4.18%
4k	7.66%	0.843%	4.21%
8k	7.51%	0.932%	4.38%
16k	7.57%	0.775%	4.52%

Table 2: Mean Relative Error (MRE) under uniform-distributed activations.

Sequence Length	FlashAttention [FP8]	INT-FlashAttention [half-INT8]	INT-FlashAttention [full-INT8]
1k	8.94%	0.317%	1.69%
2k	9.15%	0.300%	1.62%
4k	8.89%	0.280%	1.65%
8k	9.02%	0.299%	1.85%
16k	8.97%	0.296%	1.82%

5 CONCLUSION, LIMITATIONS, AND FUTURE WORK

This paper proposes INT-FlashAttention, the first token-level INT8 post-training quantization architecture compatible with FlashAttention forward workflow. We implement a INT-FlashAttention prototype with fully INT8 activations and GEMMs, which significantly improves the inference speed of FlashAttention on Ampere GPUs. The limitation of this work is that the V matrix currently is only implemented with tensor-level quantization. It remains a significant challenge to quantize V on a per-token basis. In future work, we will use per-block quantization to optimize the implementation of the V matrix. We also plan to combine our INT-FlashAttention with Hadamard transformations to further accelerate the inference process while maintaining high accuracy of the weight coefficients.

REFERENCES

- Josh Achiam, Steven Adler, Sandhini Agarwal, Lama Ahmad, Ilge Akkaya, Florencia Leoni Aleman, Diogo Almeida, Janko Altenschmidt, Sam Altman, Shyamal Anadkat, et al. Gpt-4 technical report. *arXiv preprint arXiv:2303.08774*, 2023.
- Tianqi Chen, Zhe Li, Weixiang Xu, Zeyu Zhu, Dong Li, Lu Tian, Emad Barsoum, Peisong Wang, and Jian Cheng. Ternaryllm: Ternarized large language model. *arXiv preprint arXiv:2406.07177*, 2024.
- William Dally. High-performance hardware for machine learning. *Nips Tutorial*, 2:3, 2015.
- Tri Dao. Flashattention-2: Faster attention with better parallelism and work partitioning. *arXiv preprint arXiv:2307.08691*, 2023.
- Tri Dao, Dan Fu, Stefano Ermon, Atri Rudra, and Christopher Ré. Flashattention: Fast and memory-efficient exact attention with io-awareness. *Advances in Neural Information Processing Systems*, 35:16344–16359, 2022.
- Tim Dettmers, Mike Lewis, Younes Belkada, and Luke Zettlemoyer. Gpt3. int8 (): 8-bit matrix multiplication for transformers at scale. *Advances in Neural Information Processing Systems*, 35: 30318–30332, 2022.
- Tim Dettmers, Ruslan Svirschevski, Vage Egiazarian, Denis Kuznedelev, Elias Frantar, Saleh Ashkboos, Alexander Borzunov, Torsten Hoefler, and Dan Alistarh. Spqr: A sparse-quantized representation for near-lossless llm weight compression. *arXiv preprint arXiv:2306.03078*, 2023.
- Elias Frantar and Dan Alistarh. Optimal brain compression: A framework for accurate post-training quantization and pruning. *Advances in Neural Information Processing Systems*, 35:4475–4488, 2022.
- Elias Frantar, Saleh Ashkboos, Torsten Hoefler, and Dan Alistarh. Gptq: Accurate post-training quantization for generative pre-trained transformers. *arXiv preprint arXiv:2210.17323*, 2022.
- Wei Huang, Yangdong Liu, Haotong Qin, Ying Li, Shiming Zhang, Xianglong Liu, Michele Magno, and Xiaojuan Qi. Billm: Pushing the limit of post-training quantization for llms. *arXiv preprint arXiv:2402.04291*, 2024.

-
- Changhun Lee, Jungyu Jin, Taesu Kim, Hyungjun Kim, and Eunhyeok Park. Owq: Lessons learned from activation outliers for weight quantization in large language models. *arXiv preprint arXiv:2306.02272*, 2, 2023.
- Joonhyung Lee, Jeongin Bae, Byeongwook Kim, Se Jung Kwon, and Dongsoo Lee. To fp8 and back again: Quantifying the effects of reducing precision on llm training stability. *arXiv preprint arXiv:2405.18710*, 2024.
- Shiyao Li, Xuefei Ning, Luning Wang, Tengxuan Liu, Xiangsheng Shi, Shengen Yan, Guohao Dai, Huazhong Yang, and Yu Wang. Evaluating quantized large language models. *arXiv preprint arXiv:2402.18158*, 2024.
- Yuhang Li, Ruihao Gong, Xu Tan, Yang Yang, Peng Hu, Qi Zhang, Fengwei Yu, Wei Wang, and Shi Gu. Brecq: Pushing the limit of post-training quantization by block reconstruction. *arXiv preprint arXiv:2102.05426*, 2021.
- Paulius Micikevicius, Dusan Stolic, Neil Burgess, Marius Cornea, Pradeep Dubey, Richard Grisenthwaite, Sangwon Ha, Alexander Heinecke, Patrick Judd, John Kamalu, et al. Fp8 formats for deep learning. *arXiv preprint arXiv:2209.05433*, 2022.
- Maxim Milakov and Natalia Gimelshein. Online normalizer calculation for softmax. *arXiv preprint arXiv:1805.02867*, 2018.
- Timothy Prickett Morgan. Top500 supers: This is peak nvidia for accelerated supercomputers. 2024. URL <https://www.nextplatform.com/2024/05/13/top500-supers-this-is-peak-nvidia-for-accelerated-supercomputers/>.
- Markus N Rabe and Charles Staats. Self-attention does not need $o(n^2)$ memory. *arXiv preprint arXiv:2112.05682*, 2021.
- Jay Shah, Ganesh Bikshandi, Ying Zhang, Vijay Thakkar, Pradeep Ramani, and Tri Dao. Flashattention-3: Fast and accurate attention with asynchrony and low-precision. *arXiv preprint arXiv:2407.08608*, 2024.
- Yuzhang Shang, Zhihang Yuan, Qiang Wu, and Zhen Dong. Pb-llm: Partially binarized large language models. *arXiv preprint arXiv:2310.00034*, 2023.
- Chaofan Tao, Lu Hou, Wei Zhang, Lifeng Shang, Xin Jiang, Qun Liu, Ping Luo, and Ngai Wong. Compression of generative pre-trained language models via quantization. *arXiv preprint arXiv:2203.10705*, 2022.
- Hugo Touvron, Louis Martin, Kevin Stone, Peter Albert, Amjad Almahairi, Yasmine Babaei, Nikolay Bashlykov, Soumya Batra, Prajjwal Bhargava, Shruti Bhosale, et al. Llama 2: Open foundation and fine-tuned chat models. *arXiv preprint arXiv:2307.09288*, 2023.
- Mart van Baalen, Andrey Kuzmin, Suparna S Nair, Yuwei Ren, Eric Mahurin, Chirag Patel, Sundar Subramanian, Sanghyuk Lee, Markus Nagel, Joseph Soriaga, et al. Fp8 versus int8 for efficient deep learning inference. *arXiv preprint arXiv:2303.17951*, 2023.
- Ashish Vaswani, Noam Shazeer, Niki Parmar, Jakob Uszkoreit, Llion Jones, Aidan N Gomez, Łukasz Kaiser, and Illia Polosukhin. Attention is all you need. *Advances in Neural Information Processing Systems*, 2017.
- Daliang Xu, Hao Zhang, Liming Yang, Ruiqi Liu, Gang Huang, Mengwei Xu, and Xuanzhe Liu. Empowering 1000 tokens/second on-device llm prefilling with mllm-npu. *arXiv preprint arXiv:2407.05858*, 2024.
- Zixuan Zhou, Xuefei Ning, Ke Hong, Tianyu Fu, Jiaming Xu, Shiyao Li, Yuming Lou, Luning Wang, Zhihang Yuan, Xiuhong Li, et al. A survey on efficient inference for large language models. *arXiv preprint arXiv:2404.14294*, 2024.